2022 IEEE 18th International Conference on Automation Science and Engineering (CASE)
August 20-24, 2022. Mexico City, Mexico

Quasi-static Walking for Biped Robots with a Sinusoidal Gait

Shuangfei Wu, Changliang Wang, Linqi Ye, Xueqian Wang, Houde Liu, Bin Liang

2022 IEEE 18th International Conference on Automation Science and Engineering (CASE) | 978-1-6654-9042-9/22/$31.00 ©2022 IEEE | DOI: 10.1109/CASE49997.2022.9926469

Abstract— **The quasi-static gait is a common walking strategy for legged robots. It can make the legged robots adapt to many structured terrains. Many researchers focus on the quasi-static gait for Quadruped Robots which show great efficiency and simplicity. But when applied to biped robots, the stability analysis and the gait planning are still two challenging issues. This paper focuses on the quasi-static gait for biped walking. A novel gait with the sinusoidal movement of the center of gravity is proposed to achieve smooth and fast quasi-static walking. Based on the relationship of ZMP and COG, we proposed a stability criterion for quasi-static walking and a method that adjusts the parameters of the walking pattern to achieve fast walking. The proposed method is validated by simulation analysis in VREP software. The results show that biped robots can have well-performed on flat ground.**

I. INTRODUCTION

Recently, legged robots have attracted extensive attention in the field of mobile robots due to their remarkable adaptability to complex terrains, compared to wheeled and track-based robots. Among several common kinds of legged robots, such as biped robots, quadruped robots, and hexapod robots, the biped robots show wide application potentials and research interests because of their ability to easily adapt to the environment designed for human beings. However, it is difficult to control biped robots keeping balance, especially in complex working scenarios.

To achieve stable walking for biped robots, the efforts can be made from the following aspects, such as gait planning, balance control, topographic planning, structural design, dynamic modeling, etc. Among them, gait planning is an effective strategy. While maintaining the stability of the robot is the key requirement for gait planning.

Usually, the gait using the zero moment point (ZMP) method is quasi-static gait. A biped robot is statically stable if the vertical projection of the ZMP point of the robot is within the support polygon. We can achieve stable biped walking by planning the trajectory of the Center of gravity (COG). Many researchers use the ZMP and COG to judge the walking stability [1]-[4]. For quasi-static gaits, the COG, ZMP, or center of pressure (COP) are common analysis methods [5]-[6]. These methods use a complex algorithm to achieve stability, as a matter of fact, we can also use a simple way to calculate the difference between COG and ZMP and get a novel simple gait.

*S. Wu, L. Ye, X. Wang, H. Liu are with the Center for Artificial Intelligence and Robotics, Tsinghua Shenzhen International Graduate School, Tsinghua University, 518055, Shenzhen (e-mail: {WuSF20, ye.linqi, wang.xq, liu,hd} @mails.tsinghua.edu.cn). X. Wang is the correspondent writer for his contribution.

C. W is with Shanghai Academy of Spaceflight Technology 201109, Shanghai (email:sastty@163.com)

B..Liang is with the Navigation and Control Research Center,Tsinghua University, Beijing 10084,China(e-mail:bliang@tsinghua.edu.cn)

Besides stability, walking speed is also widely studied. Researchers often change walking speeding by changing the gait features such as gait period and step length. Changing the speed with a high frequency may incur some instability, Gatesy pays attention to several species' walking patterns, observes their stride frequency, stride length, duty factor, limb excursion and proposes a controller to adapt to changing speed[7]. Compared with Gatesy's multi-gaits method, walking speed transition can be achieved by changing the parameters of our gait. Hu Y designs a controller based on the feedback for the case of walking in complex environments, a scheme is developed by adjusting the walking parameters such as stride and walking speed [8]. To ensure stable walking, optimization algorithms have been used to find suitable parameters. M. Wang uses the genetic algorithm (GA) which is carried out considering the stability and speed to optimize the walking gait parameters in [9]. GA can also optimize the path planning for biped walking and torque control architecture to improve biped control [10]. By combing the Fourier series formulation with coefficients tuning, GA can provide a way to adjust the stride-frequency, step-length, or walking pattern in real-time [11]. In this paper, speed transition can be achieved by parameters adjustment. And a simple but useful strategy is proposed to achieve speed transition.

In summary, the main contributions of the paper are as follows:

(1) A novel gait with the sinusoidal movement of the center of gravity is proposed for biped robots to achieve smooth and fast quasi-static walking.

(2) A stability criterion is derived to keep the zero moment point within the support polygon, which specifies the parameter range that ensures stable quasi-static walking.

(3) Parameter optimization is investigated to maximize the walking speed and achieve smooth speed regulation, which is verified through several simulations run.

The rest of the paper is organized as follows, Section II introduces the main results, including the relationship between the ZMP point and the vertical projection of COG, a new optimizing method for gait planning, and an algorithm for the transition for walking speed. In Section III, the proposed method is validated on several selected tasks by simulation. The conclusion is given in Section IV.

II. MAIN RESULTS

A. Relationship between COG and ZMP

ZMP is the common method to analyze the stability of quasi -static walking. For 2D plane walking, the moment of exter nal force to the ZMP is zero. As for 3D walking, ZMP refers to the point which makes the horizontal moment zero. The

relationship between ZMP and COG is given by the following derivations. The resultant force of gravity and inertial force of robots are as follows.

$$\boldsymbol{F} = \begin{bmatrix} F_x \\ F_y \\ F_z \end{bmatrix} = -\sum_{i=1}^{n} m_i \begin{bmatrix} \ddot{x}_i \\ \ddot{y}_i \\ \ddot{z}_i + g \end{bmatrix} \tag{1}$$

where m_i refers to the mass of i-th connecting rod, g refers to gravitational acceleration and $\ddot{x}_i$, $\ddot{y}_i$, $\ddot{z}_i$ represents the 3-dimensional accelerations of the ith connecting rod.

The next step is to consider the definition of ZMP point, The resultant moment of F can be represented by (2).

$$\boldsymbol{M} = \begin{bmatrix} M_x \\ M_y \\ M_z \end{bmatrix} = -\sum_{i=1}^{n} m_i \begin{bmatrix} (\ddot{z}_i + g) y_i - \ddot{y}_i z_i \\ \ddot{x}_i z_i - (\ddot{z}_i + g) x_i \\ \ddot{y}_i x_i - \ddot{x}_i y_i \end{bmatrix} \tag{2}$$

Make the first two items of (2) to be zero, the ZMP is given by (3), where x_{zmp} and y_{zmp} respectively represent the x and y coordinate of the ZMP

$$\begin{cases} M_x - F_z y_{zmp} = 0 \\ M_y - F_z x_{zmp} = 0 \end{cases} \tag{3}$$

Equation (4)represents the final results for the ZMP point.

$$\begin{cases} x_{zmp} = \dfrac{\sum_{i=1}^{n} m_i (\ddot{z}_i + g) x_i - \sum_{i=1}^{n} m_i \ddot{x}_i z_i}{\sum_{i=1}^{n} m_i (\ddot{z}_i + g)} \\ y_{zmp} = \dfrac{\sum_{i=1}^{n} m_i (\ddot{z}_i + g) y_i - \sum_{i=1}^{n} m_i \ddot{y}_i z_i}{\sum_{i=1}^{n} m_i (\ddot{z}_i + g)} \end{cases} \tag{4}$$

Assuming the height of the robot is constant, (4) can be simplified as (5)

$$\begin{cases} x_{zmp} = x - \dfrac{z\ddot{x}}{g} \\ y_{zmp} = y - \dfrac{z\ddot{y}}{g} \end{cases} \tag{5}$$

Denote x, y and z as the x, y, z position of the center of mass (COM) and z is a constant.

In a uniform gravity field, COG equals to the COM. Equation (5) describes the relationship between COG and ZMP, some useful information can be extracted from it. First, when robots take a static motion whose acceleration is zero, COG equals to ZMP. Second, to keep the ZMP inside the support polygon which is the convex hull of the robot part in contact with the ground, we should make the motion amplitude of ZMP as small as possible. It is easy to find that by taking a smaller height constant z, the motion amplitude is reduced which implies the enhancement of stability. This is consistent with the engineering experience that the robot needs to lower its height to prevent falling. Third, when we plan the trajectory of the COG for quasi-static walking, we need to use (5) to calculate the ZMP position and make it inside the support polygon to achieve stability.

B. Stability criterion for COG planning

In our method, the sine curve is chosen for COG planning because of the differentiable and easy realization. Designing other curves such as the polynomial that satisfy the acceleration and velocity limit is difficult. The poor tracking effect also brings a challenge to designing.

$$\begin{cases} x_{COG}(t) = at \\ y_{COG}(t) = b\sin(ct) \end{cases} \tag{6}$$

Equation (6) represents the desired COG trajectory where *a*, *b*, and *c* are pending parameters that can be adjusted. Parameter *a* represents the forward velocity of robots, also called the velocity factor. Parameter *b* controls maximum lateral deflection, also called the lateral deflection factor. Parameter *c* is determined by the frequency, also called the frequency factor. We assume support polygon region boundary is as follows:

$$\begin{cases} X_{\min} \le x \le X_{\max} \\ Y_{\min} \le y \le Y_{\max} \end{cases} \tag{7}$$

Equation (7) represents a typical constraint for support polygon. $X_{\max}$, $Y_{\max}$ represent the upper bound of support polygon, while $X_{\min}$, $Y_{\min}$ represent the lower bound. They can be calculated by the position and size of a biped robot foot. The assumption is suitable because almost all biped feet can be seen as a rectangle when touching the ground.

By using (5) we can calculate the ZMP position as

$$\begin{cases} x_{COG}(t) = at \\ y_{COG}(t) = (1 + \dfrac{zc^2}{g}) b\sin(ct) \end{cases} \tag{8}$$

By comparing (8) with (6), we can easily find that if the desired COG curve is a sine curve, the ZMP curve is also a sine curve that has the same frequency and phase. The difference is that the ZMP curve has a bigger amplitude, which can be seen in Fig. 1. The yellow areas represent the feet that are contacted with the ground. In a single support phase, only one area needs to be considered. It should be noted that the beginning positions of COG and ZMP are both the origin for the symmetry of biped robots and the two feet, one front and one back are foot drop sequences when walking. When biped robots walking, the center of the feet is often seen as origin, with the feet 90° phase lead or lag. The position of the foot relative to the center will be either $\frac{dx}{4}$ or $-\frac{dx}{4}$. The red curve represents the trajectory of ZMP while the blue one represents the projection of COG. The star curve means the robot is in the double support stance phase which has two support legs and a much bigger support polygon than the single one. We can find out that the curves out of the

yellow areas are all star-type (double support stance) to ensure the stability of walking. The maximum bias between ZMP and COG is $\frac{zbc^2}{g}$ which is also shown in Fig. 1.

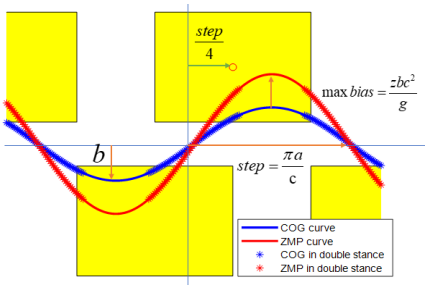

Fig. 1 The relationship between COG and ZMP for quasi-static walking. Areas in yellow represent the support polygons.

For biped robots, it is easy for the robots to keep stable in the double support phase because of the larger support polygon. So the stability of walking is determined by the stability in the single support phase. That is to say, the stable criterion of biped robots is that the ZMP satisfies condition (7) in the single support phase.

Let T represents the total time of the single support leg state in one period, s represents the y bias of the foot center in Fig. 1 and dx represents the stride. We also define a factor β that represents the magnification between single support time and double support time $\beta = \frac{T_d}{T}$. The total period time is T(1+β).

So the double support stance lasts for βT time, β is close to 0. Using (7) and (8) we get the upper bound for the sine COG curve as follows.

$$\begin{cases} \frac{aT}{2}(1+\beta) \le \frac{L}{2} + \frac{dx}{4} \\ (1+\frac{zc^2}{g})b \le \frac{W}{2} + s \end{cases} \tag{9}$$

The upper of (9) implies the upper constraint for stride. L represents the length of the foot and W represents the width. Biped robots take two steps in one period (one for the left leg and another for the right), so T/2 is used. For quasi-static walking, the stride can't exceed the $\frac{L}{2} + \frac{dx}{4}$.The second inequation of (9) represents the upper limit of the amplitude of sinecure. For a period walking, there exists another constraint between the frequency parameter c and T as (10) because the bias of y must return to 0 after a one- period walking.

$$cT(1+\beta) = 2\pi \tag{10}$$

Equation (10) tells when choosing a fixed c parameter, the period time is also fixed.

For the lower bound of the stability, we have:

$$\begin{cases} \frac{aT}{2}\beta \ge \frac{dx}{4} - \frac{L}{2} \\ (1+\frac{zc^2}{g})b\sin(\frac{c\beta T}{2}) \ge s - \frac{W}{2} \end{cases} \tag{11}$$

Based on (9) and (11), it is found that the ZMP position must be inside the support polygon in all the single support stance phases to keep balance. Fig. 1 also tells this information, all the curves without stars are in yellow areas to keep balance.

Similar to (10), there is also a relationship among the velocity parameter a, period time T, and stride dx.

$$a(1+\beta)T = 2dx \tag{12}$$

Substituting (10) and (12) into (9) and (11) we can rewrite the stability criterion:

$$\begin{cases} \pi a \le \frac{2}{3}cL \\ (1+\frac{zc^2}{g})b \le \frac{W}{2} + s \\ \pi a(\frac{1}{2} - \frac{2\beta}{1+\beta}) \le cL \\ (1+\frac{zc^2}{g})b\sin(\frac{\beta\pi}{1+\beta}) \ge s - \frac{W}{2} \end{cases} \tag{13}$$

Compared with the first inequation, the third one of (13) can be ignored. This tells us when the frequency of walking is fixed, the velocity has an upper boundary but no lower boundary. The minimum value of parameter a is 0, which corresponds to the situation of standing still. When taking fixed X_{max}, and Y_{max} .we can draw the constraints among the parameters as Fig. 2. When we plan the trajectory of COG, we need to consider the limit to keep stability.

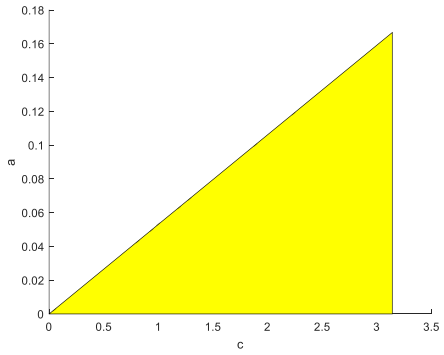

(a) Yellow area: the feasible range for a, c that ensures the quasi-walking is stable

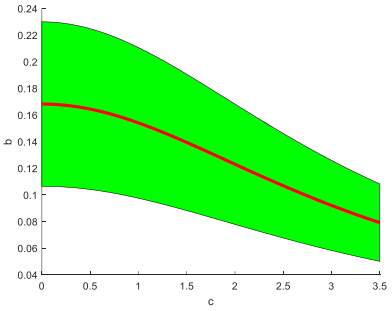

(b) Green area: the feasible range of *b*, *c*, which ensures the quasi-walking is stable; Red line: the red centerline is applied in our controller to maximize the stability

Fig. 2 The constraints among the parameters for stable walking. The sub-picture (a) shows the velocity-frequency (a-c) constraint range value and (b) is lateral deflection-frequency (b-c). Here we choose g=9.8, z=0.9, L=0.25 W=0.2, s=0.13

Fig. 2(a) tells that to achieve high-speed walking, we need to set frequency parameter *c* as big as possible to increase the value range of velocity parameter *a*. Fig. 2(b) reminds us that if frequency parameter *c* is too big, the selection of *b* will be difficult for the reduced range when increasing *c*.

To obtain a stable sinusoidal gait curve, how to design an appropriate parameter *b* is urgent. There is a simple and efficient strategy which is the arithmetic mean of upper and lower bounds of feasible reason. Simulation has proved that the strategy is indeed effective.

$$b = \frac{W/4 + s/2}{(1+\frac{z}{g}c^2)} + \frac{s/2 - W/4}{(1+\frac{z}{g}c^2)\sin(\frac{c\beta T}{2})} \qquad (14)$$

(14) tells us when frequency parameter *c* is set, we can set *b* in the middle of its feasible range to keep balance. The simulation will prove the effectiveness of this selection.

C. *Quasi-static gait planning*

Based on the stability criterion of COG planning given above, a novel quasi-static gait planning method is proposed. The planning process is as follows:

First, we analyze the walking process. The biped walking process can be divided into four parts:

(a) Move the COG to the right, lift the left leg and put the left leg onto the desired position. At this time, the left leg is the swing leg and the right leg plays the role of support leg, with the right foot touching the ground providing the support polygon.

(b)Move the COG to the middle position. Ensure the ZMP point in the support polygon at the same time. When the left leg touched the ground, there exists a short time that both the legs play the support leg.

(c)Move the COG to the left and lift the right leg, do symmetrically as mentioned above.

(d)Double support legs state which lasts for a short time. The above process is shown in Fig. 3. The position of the COG projection is shown in Fig. 1.

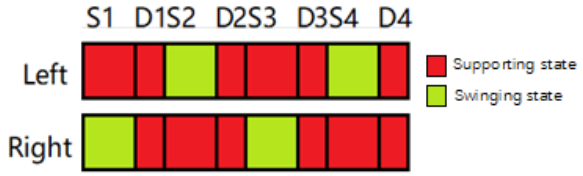

Fig. 3 The supporting leg transition during our biped walking

In Fig. 3, S means the single support leg time while D means the double support legs time which is short but can't be negligible. The red area means the leg is acting as the support leg while the green means the swing leg. We can see both the legs are touching the ground when in D state. It should be noted that we draw the double stance phase for this length only for illustrating the phase, not standing for lasting for such a long time.

For faster walking, we need to optimize the parameters of the walking patterns. First, we analyze the speed relationship. Parameter *a* is determined by the stride and period time. We can accelerate walking by using a bigger step or smaller period times. We also need to choose the parameters that are satisfied with the (13) inequations.

We can calculate the max speed for quasi-static walking:

$$V_{\max} = \frac{dx}{dt} = a \qquad (15)$$

(13) and (15) tell us that the higher frequency, the longer stride, the faster speed. (13) also tells the bias of the y-axis can be decreased with frequency parameter *c* increase. If the frequency of walking is large enough, *b* is small enough which can be seen as zero, then the biped robots can walk without lateral displacement. In fact, we can not choose *c* as large as possible due to the limit of motors and *a* also has an upper bound.

We can always set velocity parameter a to zero when *b* and *c* are fixed, meaning the minimum speed is zero.

D. *Speed transition*

In many cases, it is necessary to change the walking speed of robots. And the speed can be controlled by choosing different planning parameters. So, the transition of parameters to achieve speed control is discussed below.

(15) tells that only velocity parameter *a* as a direct influence on the walking speed. To realize the smooth change of speed. We develop a controller to regulate parameter *a*.

$$a_{k+1} = \beta a_k + (1-\beta)a_{target} \qquad (16)$$

Here β is the accelerating factor between 0 and 1. By using (16), The transition of *a* is smooth and the biped robot will slowly change its speed to the target.

However, the constraints (13) tells that the value of *a* can't be set freely. If the target speed is too big, a biped robot can not have a stable walking at the target speed with the fixed -parameters *b* and *c*. We need to increase the frequency parameter *c* to expand the range of *a*. This operation will cause the feasible range of *b* reduced which can be seen in Fig.

2(b). To solve the problem, we propose the algorithm as Fig. 4:

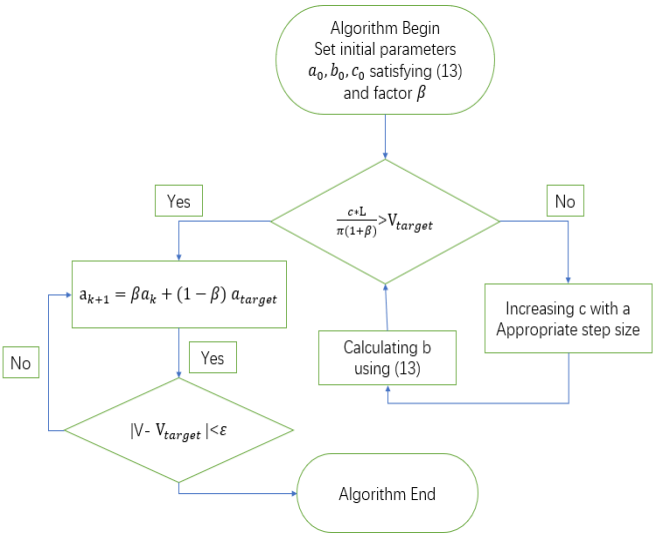

Fig. 4 The algorithm for the speed transition

We can achieve a smooth transition of speed by using the algorithm in Fig. 4.

The stability of speed transition should also be considered because the distance from the drop point to the center would also change with the speed variations. Then we rewrite the stability criterion (9)(11) as follows.

$$\begin{cases} \dfrac{aT_k}{2}(1+\beta) \le \dfrac{L}{2} + \dfrac{dx_{k-1}}{4} \\ (1+\dfrac{z}{g}c_k^2)b \le \dfrac{W}{2} + s \\ \dfrac{a\beta T_k}{2} \ge \dfrac{dx_{k-1}}{4} - \dfrac{L}{2} \\ (1+\dfrac{z}{g}c_k^2)b\sin(\dfrac{c_k \beta T_k}{2}) \ge s \end{cases} \tag{17}$$

The difference between (17) and (13) is the parameters and stride are time varying. When the biped robot lifts its leg and prepares the next new step, the support leg is still in the previous configuration. This phenomenon is caused by the discrete control of the biped robots. We can use (17) to replace the (13) in Fig. 4 to improve the algorithm and solve the problem.

III. Simulation Results

We use a simplified biped robot model in VREP to test the effectiveness of our method. Table I shows the robot parameters. Fig. 5 shows the front view and side view of the biped model.

The biped robot in simulation has a body weight of 0.4kg without any arms or shoulders. Each leg has 6 degree of freedom which can provide the desired COG motion.

The simulation parameters are introduced as TABLE I.

TABLE I The Parameters Of The Biped Model

Quantity	VALUE	Quantity	VALUE
Body width	0.1m	Foot length	0.07m
Height	0.3m	Foot width	0.05m
Joints number	12	Body width	0.1m
Leg length	0.1m	Mass(total)	0.6kg

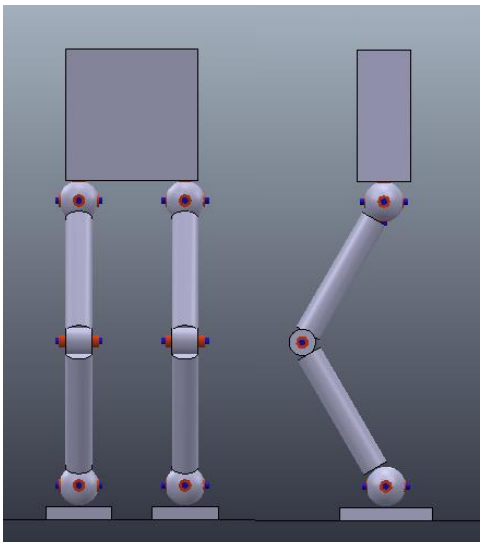

Fig. 5 The front view and right side view of our biped model

A. The max walking speed simulation

In our biped model, W=0.05m, L=0.07m, we set s=0.065m, z= 0.3m, g=9.8m/s^2 β=0.1. From (13), we can choose suitable parameters to get the target speed. As for the max walking speed, it is estimated by a large number (over 500 times) of simulation experiments. The maximum speed is 0.11 m/s when a = 0.1667, b=0.0297, and c = 2π..

The simulation result is as shown in Fig. 6, which depicts the front view and side view of the biped model walking at a certain speed.

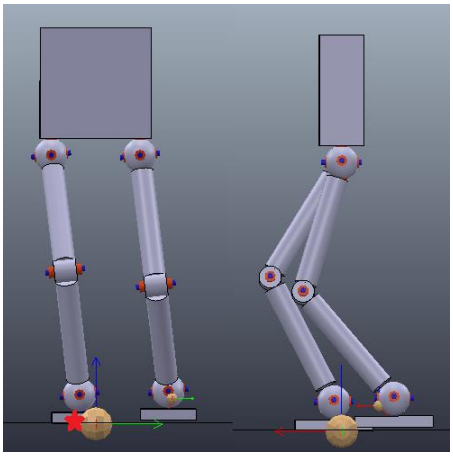

Fig. 6 The simulation when walking at a speed =0.11 m/s. The virtual circular point on the ground is the projection of COG. The star is the ZMP point we calculated which is also a virtual point. From the side view, the ZMP is obscured by the projection of COG

The position of the COG projection can be seen in Fig. 7 and the position and velocity of COG are shown in Fig. 8.

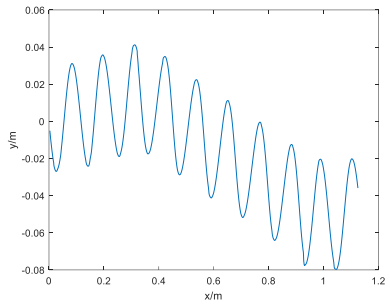

Fig. 7 The COG projection when walking at a speed of 0.11m/s

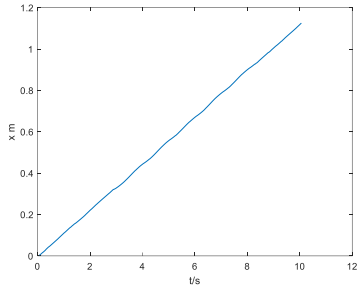

(a)The x position of COG when walking at a speed of 0.11m/s

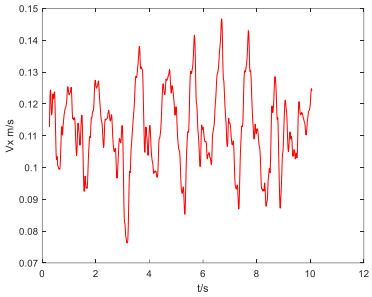

(b) The x velocity of COG when walking at a speed of 0.11m/s

Fig. 8 The x transition of COG projection with time. The sub-figure (a) shows the relationship between position and time while the sub-figure (b) shows the velocity and time

As is shown in Fig. 7, approximately the COG projection is moving along a predetermined sinusoidal trajectory. The reason for the deviation from expectation is the error of the model. This effect will have a significant reduction when walking at low speed. In fact, the mass of the body is 0.4 kg while the other parts weigh 0.2 kg in total which means the point-mass model is improper. The orientation of the body also has an influence on the track. Fig. 8(b) tells that the speed of the biped is about 0.11 m/s. The fluctuation of speed is caused by the disturbance and sensor error. It should be noted that lateral defection does not have an effect on the speed which is shown in (15). It only influences stability. To accelerate the biped, we can use larger c and a, but the larger c is, the smaller value range of b, which brings challenges to the selection of b and the robustness. Also, the maximum torque of the motor sets a boundary for a and c. Through many experiments, we find the 0.11 m/s is the fastest speed. Accelerating the biped further will cause instability. By comparison, Nao, a biped robot whose height is about 0.58m can only walk at a speed of 0.075 m/s in V-REP simulation. Asti and Marty in simulation can't walk faster than ours, either. The walking speeds in simulation are as TABLE II. From TABLE II, we can calculate the speed height ratio, which can be an evaluation index for the speed performance. For our algorithm, the ratio is 0.37 which is bigger than the robots below.

TABLE II THE WALKING SPEED OF BIPED ROBOTS IN V-REP

Robot	Height	Max speed
Asti	1.2m	0.075m/s
Marty	0.2m	0.01m/s
Nao	0.45m	0.075m/s

B. The speed transition simulation

Two simulation tasks are used to display the effect of speed transition. One accelerating process from zero to 0.05 m/s, One slowing process from 0.05 m/s to zero. The simulation results are shown in Fig.9 and Fig.10 respectively.

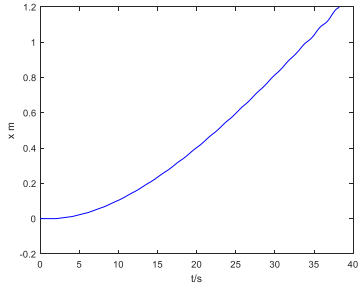

(a)The x position of COG when accelerating from 0 to 0.05 m/s

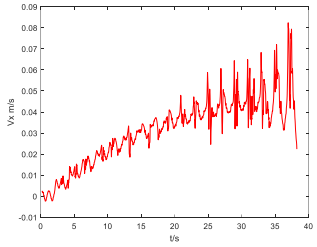

(b)The x velocity of COG when accelerating from 0 to 0.05 m/s

Fig. 9 The x transition of COG projection with time when accelerating from 0 to 0.05 m/s

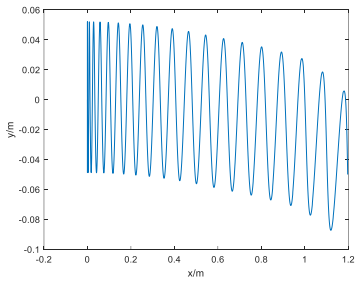

Fig. 10 The relationship between x position and y position of COG when accelerating from 0 to 0.05 m/s

In Fig. 9, we use $a_{k+1} = 0.9a_k + 0.1a_{target}$ to update the speed. The speed of the biped robot increases evenly which can be seen from the shape of the curve in Fig. 9(a) which approximates the shape of a parabola. We can see the initial speed of the biped robot is zero for the zero slopes of the curve at origin. This information can also be confirmed through Fig. 10. At the beginning time, the biped robot stands still resulting in the coincident curves in the left part of Fig. 10. Fig. 9(b) tells the final velocity is about 0.05 m/s after accelerating.

For the deceleration case, it seems that we can do this by making the velocity parameter zero at once which is an easier and faster way to stop the biped robot. In fact, this strategy can not work well when the lateral deflection is big enough because it does not satisfy the third item of (17). Fig. 11 shows the falling situation.

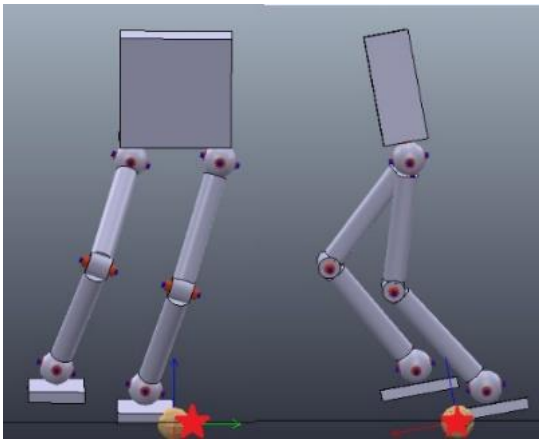

Fig. 11 The time when the biped robot is falling. The circular point represents the projection of COG and the star stands for the ZMP.

From Fig. 12, we can see when the robot is taking in-place walking with a speed of zero, the feet are not parallel to the body.

To achieve a fast and stable stopping, we use $a_{k+1} = 0.5a_k + 0.5a_{target}$ as the control strategy to reduce the slow deceleration time.

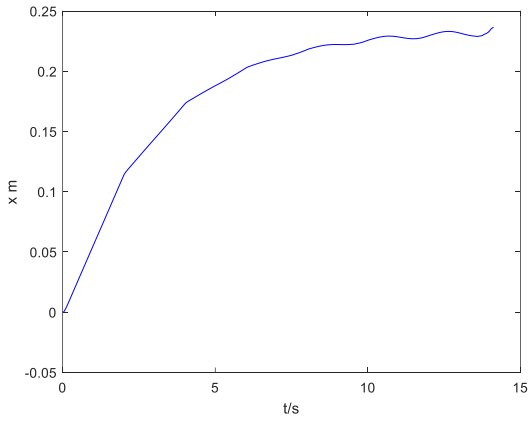

(a) The x position of COG when decelerating from 0.05m/s to 0

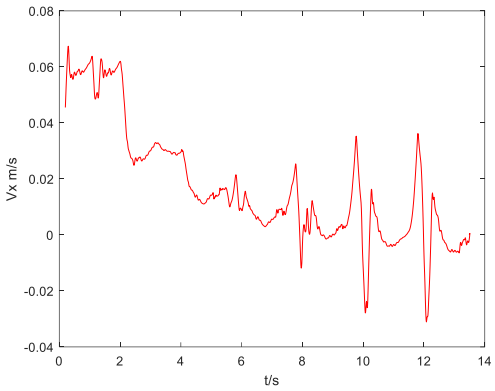

(b) The x velocity of COG when decelerating from 0.05m/s to 0

Fig. 12 The x transition of COG when decelerating from 0 to 0.05 m/s

Fig. 12 shows the x position of COG when the biped robot is stopping. Compared with Fig. 9, Fig. 12 shows that the stopping process is much faster than the accelerating process. It is because we use a smaller accelerating factor β =0.5.

The x-y position of COG is shown in Fig. 13.

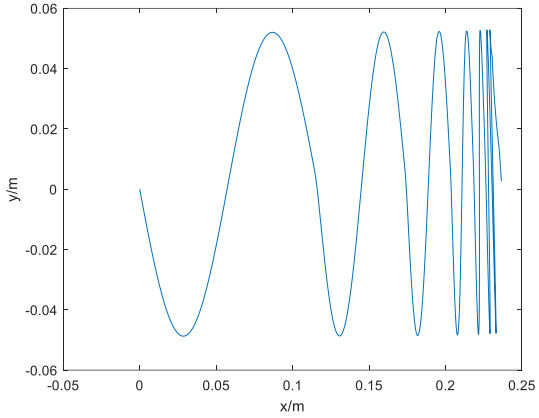

Fig. 13 The x-y position of COG when decelerating from 0 to 0.05 m/s

From the right part of Fig. 13, we can see the biped robot take an in-place walking finally which shows the forward speed is 0.

IV. Conclusion

In this paper, we discussed the relationship of ZMP and COG for biped robots and proposed the stability criterion for COG planning that ensures stable quasi-static walking. Then, we proposed a novel method for sine curve COG planning to achieve smooth and fast quasi-static walking. The simulation results validated the effectiveness of our methods. The biped robot can walk at least one third faster than the other biped robots in V-REP simulation.

For further research, we will apply the proposed method to a real biped robot to possibly improve its walking speed as well as stability.

REFERENCES

[1] Kim, S., Hirota, K., Nozaki, T., & Murakami, T. "Human motion analysis and its application to walking stabilization with Cog and ZMP." *IEEE Transactions on Industrial Informatics*, vol 14, no 11, pp 5178-5186, 2018

[2] Yamamoto, T. &Sugihara, T. "Foot-guided control of a biped robot through ZMP manipulation." *Advanced Robotics* vol 2, pp 1472-1489, 2020

[3] T. Ando, T. Watari and R. Kikuuwe, "Reference ZMP Generation for Teleoperated Bipedal Robots Walking on Non-Flat Terrains," *2021 IEEE/SICE International Symposium on System Integration (SII)*, 2021, pp. 794-800

[4] T. Sugihara, K. Imanishi, T. Yamamoto and S. Caron, "3D biped locomotion control including seamless transition between walking and running via 3D ZMP manipulation," *2021 IEEE International Conference on Robotics and Automation (ICRA)*, 2021, pp. 6258-6263,

[5] J. Yu, Y. Liu, R. Li, G. Zuo and N. Yu, "Stable Walking of Seven-link Biped Robot Based on CPG-ZMP Hybrid Control Method," *2021 IEEE International Conference on Robotics and Biomimetics (ROBIO)*, 2021, pp. 870-874

[6] Ringhof, S., Stein, T, Potthast, W., Schindler, H. J., & Hellmann, D. "Force-controlled biting alters postural control in bipedal and unipedal stance." Journal of oral rehabilitation, vol 42, no 3, pp 173-184, 2015

[7] Gatesy, S. M., & Biewener, A. A. "Bipedal locomotion: effects of speed, size and limb posture in birds and humans."Journal of Zoology, vol 224, no 1, pp 127-147, 1991

[8] Hu, Y., Yan, G., & Lin, Z." Feedback control of planar biped robot with regulable step length and walking speed." IEEE Transactions on Robotics, vol 27, no 1, pp 162-169. 2010

[9] M. Wang, R. Wang, J. Zhao and P. Sun, "An Optimized Algorithm Based on Energy Efficiency for Gait Planning of Humanoid Robots," *IECON 2018 - 44th Annual Conference of the IEEE Industrial Electronics Society*, pp. 5612-5617, 2018

[10] A. Vedadi, K. Sinaei, P. Abdolahnezhad, S. S. Aboumasoudi and A. Yousefi-Koma, "Bipedal Locomotion Optimization by Exploitation of the Full Dynamics in DCM Trajectory Planning," *2021 9th RSI International Conference on Robotics and Mechatronics (ICRoM)*, pp. 365-370 2021

[11] L. Yang, C. M. Chew, A. N. Poo and T. Z, "Adjustable Bipedal Gait Generation using Genetic Algorithm Optimized Fourier Series Formulation," *2006 IEEE/RSJ International Conference on Intelligent Robots and Systems*, pp. 4435-4440,2006